Heliyon 9 (2023) e15743

Contents lists available at ScienceDirect

Heliyon

journal homepage: www.cell.com/heliyon

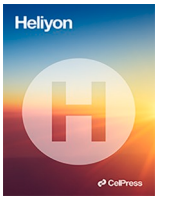

Research article

Biogenic synthesis of *RICINUS COMMUNIS* mediated iron and silver nanoparticles and its antibacterial and antifungal activity

V.K. Linima *, R. Ragunathan, Jesteena Johney

Department of Biotechnology (Bionanotechnology), Centre for Bioscience and Nanoscience Research, Eachanari, Coimbatore - 21 , Tamilnadu, India

ARTICLE INFO

Keywords:
Iron and silver nanoparticles
GC-MS
SEM
Anti-microbial activity
MIC

ABSTRACT

In recent years, many strategies have been developed for the biological synthesis of different types of metal nanoparticles, which have been successfully synthesized from various plant extracts and analyzed. Recent studies have demonstrated that nanoparticles have highly promising antimicrobial, antiviral, and anti-cancer properties. In the present study, biological synthesis of *Ricinuscommunis* leaves was performed with iron and silver nanoparticles. The synthesized iron and silver nanoparticles were characterized by UV–Vis spectroscopy, Fourier transform infrared (FT-IR), X-Ray Diffraction (XRD), Scanning electron microscopy (SEM) with Energy dispersive spectroscopy (EDS), and Transmission electron microscopy (TEM). GC-MS analysis of the *Ricinus communis* revealed the secondary metabolites of total phenolic and flavonoid contents of the extract, which are responsible for the bio-reduction reaction during nanoparticle synthesis. The UV–Vis spectrum shows Plasmon peaks at 340 nm and 440 nm for iron and silver nanoparticles, respectively. XRD results revealed crystalline structure, while TEM, SEM, and EDS identified iron and silver with mostly cuboidal and spherical shapes. Antimicrobial activity was also performed, and it was found that both nanoparticles were active against *Salmonella typhi* (6 ± 0.073) and (7 ± 0.040), *Staphylococcus aureus*, and *Aspergillus flavus*. MIC was also performed, and AgNPs gave a better bactericidal effect against *Staphylococcus aureus*.

1. Introduction

Nanotechnology deals with the branch of science that manipulates matter at the atomic or molecular scale [1]. Nanoparticles have one dimension in the size range of 1–100 nm, serving as a bridge between atomic or molecular structures and bulk materials [2]. Nanoparticles have gained attention due to their unique morphological and physicochemical properties [3]. These metal nanoparticles possess strong inhibitory and antibacterial activity [4]. Iron nanoparticles have been widely applied in drug delivery and biomedical applications and possess toxicity against a broad spectrum of pathogenic bacteria and fungi [5]. Silver nanoparticles possess heterogeneity of beneficial properties, such as electrical conductivity, optical and biological properties. Green synthesis of silver nanoparticles is cost-effective and non-toxic, and they exhibit high stability, solubility, and antibacterial properties [6].

Green nanotechnology integrates the use of plant elements to ensure a field with good safeguarding of the safety of life. It is a favourable application in the field of nanotechnology, reducing dangers while improving the environment's resilience [7]. Metal nanoparticles are synthesized for various applications using extracts of different plant parts such as flowers, leaves, seeds, and roots [8]. Biological synthesis utilizes plant extracts, exudates, and inactivated plant tissue [9]. Therefore, plant-based biogenic synthesis of nanoparticles has antibacterial potency due to affluent sources of metabolites with medicinal properties [10]. Iron and silver

* Corresponding author.

https://doi.org/10.1016/j.heliyon.2023.e15743
Received 1 January 2023; Received in revised form 19 April 2023; Accepted 20 April 2023
Available online 23 April 2023

nanoparticles have been synthesized using numerous plants [11], such as *Erodium cicutarium* [12] and *Nerium oleander* [13]. Among these plants, *Ricinus communis* (castor) is a flowering plant used as an antioxidant, fungicide, antiulcer, wound healer, laxative, antiasthmatic, and insecticide agent. This is due to the presence of alkaloids, flavonoids, steroids, saponins, glycosides, etc. [14].

In the present study, iron and silver nanoparticles were biologically synthesized using *Ricinus communis* (castor), and they were characterized by UV–Vis absorption spectroscopy, Fourier transforms infrared (FT-IR), X-Ray Diffraction (XRD), Scanning electron microscopy (SEM) with Energy dispersive spectroscopy (EDS) and Transmission electron microscopy (TEM). The synthesized nanoparticles were used for antimicrobial and MIC studies to identify the biomedical importance of the synthesized nanoparticles.

2. Materials and methods

2.1. Collection and identification of plant

Healthy and matured medicinal plant leaves of *Ricinus communis* (Fig. 1) were collected from the area of Eachanari, Coimbatore district, Tamilnadu. The collected plant was identified and authenticated by Dr M. U. Sharief (Scientist), Botanical Survey of India, (BSI/SRC/5/23/2022/625/December 01, 2022) Agricultural University, Tamilnadu, India.

2.2. Preparation of Ricinus communis leaf extract

Fresh leaves of *Ricinus communis* were washed thoroughly with tap water followed by distilled water to remove all the dust and air dried. About 10 g of cleaned leaves were cut into small pieces, crushed using a mortar and pestle, and mixed with 100 mL of double-distilled water to obtain an aqueous extract. Another 10 g of leaves extract was mixed with methanol and incubated at 60–70 rpm overnight. The mixture was then filtered using Whatman's No. 1 filter paper and used for further study [15].

2.3. Antioxidant assays

To determine the antioxidant potential of the aqueous extract and synthesized iron and silver nanoparticles of *Ricinus communis*, two assays were used: DPPH (1,1-diphenyl-2-picrylhydrazyl radical) and total antioxidant activity (phosphomolybdenum method) [6].

2.4. Phytochemical analysis and TLC analysis of leaf extract

Phytochemical analysis of the leaf extract of *Ricinus communis* was carried out to analyze the presence of phytoconstituents such as alkaloids, phenols, saponins, quinones, terpenoids, sugars, flavonoids, proteins, and steroids. The phytochemicals were confirmed by thin-layer chromatography (TLC) analysis, which was carried out on both aqueous and methanolic extracts of *Ricinus communis* (Castor) [16].

2.5. GC-MS analysis

GC-MS analysis is a powerful analytical technique used to identify and quantify the chemical components of a sample. In this study, it was used to analyze the bioactive compounds present in the leaves of *Ricinus communis*. The analysis was carried out using an AGILENT CH-GCMSMS-02 instrument with a total running time of 36 min. The temperature was initially set at 110 °C for 2 min and then increased at a rate of 100 °C/min to 2000 °C, followed by an increase of 50 °C/min to 2800 °C, and then held isothermal at 2800 °C for 9 min. Mass spectra were obtained at 70eV, with fragments ranging from 45 to 450 Da and a scan interval of 0.5 s. The relative percentage of each component was calculated by comparing the average peak area to the total areas [17].

Fig. 1. *Ricinus communis* leaves.

2.6. Synthesis of iron nanoparticles

A 0.1 M FeCl3·6H2O solution was prepared in double distilled water, and the aqueous leaf extract was mixed in a 1:1 ratio. The equal volume of leaf extract was added dropwise to the ferric chloride solution and stirred with a stirrer at room temperature. The appearance of a colour change in the solution from light yellow to black indicated the formation of iron nanoparticles. The obtained precipitate solution was centrifuged at 6000 rpm and washed with water, followed by drying in an oven at 60 °C [18].

2.7. Synthesis of silver nanoparticles

A 0.1 mM AgNO3 solution was prepared by dissolving 0.1698 g of AgNO3 in 1 L of double distilled water. For the fabrication of silver nanoparticles, 10 mL of plant extract was added to 90 mL of 1 mM AgNO3 in a 250 mL conical flask, and the mixture was kept in a dark place at room temperature for 48 h. The formation of silver ions to silver nanoparticles was marked by the appearance of a dark brown colour. The synthesized silver nanoparticles were separated by centrifugation at 9000 rpm for 20 min. The particles were then washed with water and 70% ethanol and dried at 60 °C before being stored for further study [19].

2.8. Characterization of the nanoparticles

2.8.1. UV–vis spectral analysis

UV–Vis analysis was carried out as the primary confirmation of the synthesized iron and silver nanoparticles using a LABTRONICS spectrophotometer (Model LT-291) over a wavelength range of 200 nm–800 nm [20].

2.9. Fourier transform infrared analysis (FT-IR)

The functional groups of the synthesized iron and silver nanoparticles were analyzed by recording their FT-IR spectra using a SHIMADZU FT-IR spectrometer over the range of 400 cm^{-1} to 4000 cm^{-1} [18].

2.10. Scanning electron microscopy (SEM) and energy dispersive spectroscopy (EDS)

The morphological features of the synthesized iron and silver nanoparticles were analyzed using a ZEISS EVO 18 scanning electron microscope. Thin film samples were coated on carbon tape copper grids, and images were recorded. The elemental composition and purity of the iron and silver nanoparticles were examined using Energy Dispersive Spectroscopy (EDS) with the ZEISS EVO 18 operated at 20 kV [9].

2.11. X-Ray Diffraction analysis (XRD)

The Panalytical Empyrean X-ray diffractometer was used to perform the crystallographic analysis of the iron and silver nanoparticles. The Debye-Scherrer equation was used to calculate the crystalline size of the nanoparticles from the diffraction peaks [21].

$$D = (K\lambda) \div (\beta Cos\theta)$$

D is the nanoparticles size, λ is the wavelength, β is the line width in radius and K is the shape of factor (constant).

2.12. TEM (transmission electron microscopy)

Transmission Electron Microscopy analyses were performed to determine the size, morphology, crystalline nature, and dispersal of the synthesized iron and silver nanoparticles. The analyses were conducted using a JEOL JEM 2100 TEM operated at 120 kV [20].

2.13. Antibacterial activity of synthesized iron and silver nanoparticles

The well diffusion method was employed to evaluate the antibacterial activity of *Ricinus communis* leaves mediated iron and silver nanoparticles. Mueller Hinton agar (3.42 g in 90 mL of distilled water, HIMEDIA-Mumbai, India) was prepared, sterilized (at 121 °C for 15 min), and poured into sterilized petri plates. The plates were allowed to solidify, after which they were swabbed with 70 μl of bacterial cultures of *Escherichia coli*, *Staphylococcus aureus*, and *Salmonella typhi*. Wells were made with a cork borer, and 20 μl samples were added. The antibiotic disc of Amikacin (AK30) was placed as a positive control. The plates were then incubated at 37 °C for 24 h, and the antibacterial activity was confirmed by measuring the zone of inhibition in mm [22].

2.14. Antifungal activity of synthesized iron and silver nanoparticles

The antifungal activity of castor leaf-mediated iron and silver nanoparticles was analyzed using the well diffusion method. Malt agar was prepared by dissolving 2.7 g in 60 mL of distilled water (HIMEDIA-Mumbai, India) and poured into sterile conditions to solidify. Pathogenic strains of *Aspergillus niger* and *Aspergillus flavus* were swabbed onto the agar. Wells were made using a cork borer (15 mm) and the samples were added, with 10 μl of fluconazole placed as the positive control. The plates were incubated at 30 °C for

3–5 days, and the zone of inhibition was measured in mm [22].

2.15. Minimum inhibitory concentration (MIC)

The antibacterial activity of the synthesized iron and silver nanoparticles was determined using a 96-well plate method. Each row of wells in sterile plates was filled with 0.1 mL of sterilized nutrient broth, and samples were added in different concentrations of 10, 20, 30, 40, and 50 μl along with 10 μl of *Staphylococcus aureus* culture. The plates were incubated at 37 °C for 24 h, and the resulting turbidity was assessed for the minimum inhibitory concentration, where growth was no longer visible, by taking optical density readings at 600 nm with a 96 ELISA plate reader (ROBONIK). The percentage of cell death was calculated using the equation [23].

$$\text{Percentage of cell death} = \frac{\text{Control OD} - \text{Sample OD}}{\text{Control OD}} \times 100$$

2.16. Statistical analysis

The standard deviation was used to compare the results of antioxidant and antibacterial activities of the synthesized iron and silver nanoparticles, where $^*p < 0.05$ was considered a significant result. The data were presented as the mean of triplicates ± standard error, and the experiment was done in triplicates.

3. Results and discussion

3.1. Antioxidant activity

The activity of DPPH and total antioxidants in the aqueous extract and synthesized iron and silver nanoparticles is shown in Table 1. The inhibition percentage for μg was observed in the aqueous extract of DPPH and total antioxidant, which were 347 ± 0.036 and 650 ± 0.074, respectively. However, iron nanoparticles were found to be 401 ± 0.016 and 636 ± 0.142 μg, while the inhibition percentage of silver nanoparticles was 397 ± 0.034 and 641 ± 0.017 μg. Kiran et al. [24] reported similar studies on the DPPH assay, in which biologically synthesized iron and silver nanoparticles exhibited inhibitions of 18.06 ± 0.60% and 20.83 ± 0.33%, respectively. Moreover, the results obtained were similar to the antioxidant property of biologically synthesized *Morinda lucida* leaves extract-mediated silver nanoparticles [25]. The synthesized nanoparticles were compared to the leaves extract of *Ricinus communis*, implying that only small amounts of nanoparticles are required for DPPH, further confirming better antioxidant activities than leaves extract. Ulewicz and Wesolowski et al. [26] reported that the increased antioxidant activity of nanoparticles relative to the raw extract was fascinating, as antioxidants protect humans from stress-related illnesses through chemoprotection.

3.2. Phytochemical analysis

The phytochemical analysis of *Ricinus communis* leaves was carried out using aqueous and methanolic extracts to determine the presence of various phytoconstituents, such as phenols, saponins, proteins, steroids, alkaloids, terpenoids, and flavonoids (refer to Table 2).

3.3. TLC analysis

The Thin-layer Chromatography (TLC) of *Ricinus communis*-mediated aqueous and methanolic extracts of various phytochemical constituents was confirmed by the Rf value of TLC. The Rf value of the aqueous extract illustrated spots at 0.5 and 0.72, while the methanolic extract showed spots at 0.4, 0.62, and 0.74. Alkaloids act as bio-reducing agents during nanoparticle synthesis. TLC analysis of the extract of six medicinal plants gave similar results for various phytochemicals with different Rf values [27].

3.4. GC-MS analysis

The GC-MS analysis of the methanolic extract of *Ricinus communis* confirmed the presence of various components with different retention times, such as Quinoxaline, 2-phenyl; Norreticuline, *N*-formyl-; Phthalic acid, 4-nitrophenyl 2-propyl ester; Fumaric acid, di (2-fluorophenyl) ester; Thiazolidin-4-one, 2-(4-methylphenylimino)-; Citronellol; Vanadium, (.eta.7-cycloheptatrienylium)(.eta.5–2,4-cyclopentadien-1-yl)-; Adamantane-1-carboxamide, *N*-[2-(3,4-dimethylphenoxy)ethyl]-; 6,7,8-Trimethoxy-3,4-dimethyl-1-

Table 1
DPPH and total antioxidant activity of aqueous extract, synthesized FeNPs and AgNPs.

Test adopted	Aqueous	FeNPs AgNPs
DPPH	347 ± 0.036	401 ± 0.016 397 ± 0.034
Total antioxidant	650 ± 0.074	636 ± 0.142 641 ± 0.017
	μg	μg μg

Table 2
Phytochemical analysis of aqueous and methanolic extracts of *Ricinus communis*.

Phytoconstituents	Test adopted	Aqueous	Methanol
Alkaloids	Mayer's test	+	+
Phenol	$FeCl_3$ test	+	−
Saponins	Foam test	+	−
Quinones	NaOH test	+	−
Terpenoids	H_2SO_4 test	−	−
Sugar	Felling's test	−	−
Flavonoids	HCl test	+	+
Protein	Folinlowry's test	+	+
Steroids	H_2SO_4 test	+	−

+:Present, −: Absent.

methylsulfanyl-3,4-dihydroisoquinoline and Thiazolidin-4-one, 2-(4-methylphenylimino) (Table 3). These components have several biological functional activities, such as antimicrobial, anticancer, antioxidant, treatment of parasitic diseases, malign tumors, viral infections, chemotherapeutic agents, anti-inflammatory, antitubercular, and antidiabetic. The compound phytol has shown various activities, including aromatic ingredient, antimicrobial, anxiolytic, metabolism-modulating, cytotoxic, and antioxidant. Upon degradation of chlorophyll, the component phytol, a diterpene alcohol, is used in the synthesis of vitamins K and E [18]. Lakshmi et al. [28] reported similar studies with the methanolic extract of *Lactucaruncinata*, where various compounds were identified with GC-MS analysis.

3.5. UV–visible absorption spectroscopy

The UV–Visible spectroscopy of *Ricinus communis* leaves-mediated iron and silver nanoparticles was confirmed Fig. 2(a and b). The UV–Vis analysis of iron and silver nanoparticles showed strong absorbance peaks at 340 nm and 440 nm, respectively. Nahid et al. [12] reported the absorption peak of *Erodium cicutarium*-mediated iron nanoparticles at 230 nm. The surface plasmon resonance (SPR) of silver nanoparticles showed a peak at 420 nm. Furthermore, the SPR band for silver nanoparticles obtained the absorbance peak at 430 nm, as reported in previous studies [14]. Similarly, Monika et al. [4] reported that silver nanoparticles prepared using a plant extract exhibited a strong plasmon peak at 429 nm. The band intensity produced by silver nanoparticles was identified as a peak due to the surface plasmon resonance, which is an intrinsic property of metal band-based nanoparticles. These important findings regarding the potent antioxidant potential of silver nanoparticles are similar to those of previous studies on biosynthesized silver nanoparticles [29].

3.6. Fourier transform infrared (FT-IR) spectroscopy

Fourier transform infrared spectroscopy (FT-IR) was used to analyze the chemical composition of organic chemicals of *Ricinus communis*-mediated iron and silver nanoparticles [Fig. 3(a and b)]. The FeNPs showed absorbance bands at 408.91, 447.49, 470.63, 516.92, 547.78, 624.94, 648.98, 1010.70, 1080.14, 1149.57, 1234.44, 1442.75, 1527.62, and 1643.35 cm^{-1}. Additionally, two peaks were observed in the spectrum of green-synthesized iron nanoparticles: 1527.62 cm^{-1} related to a strong amide CO group and 1643.35 cm^{-1} related to CC aromatic. These results are consistent with Sravanthi et al. [30], who reported the amide peak (protein) responsible for the immobilization of FeNPs, and Edwin et al. [18], who reported OH vibrational frequencies, C–O–C, and metal oxygen as the cause of these peaks. The AgNPs are illustrated in the FT-IR spectrum and showed absorbance bands at 3842.20, 3718.76, 3525.88, 1743.65, 1643.35, 1033.85, 686.66, and 547.78 cm^{-1}. The peak at 1033.85 cm^{-1} is related to a strong C–OH group, 3718.76 cm^{-1} observed strong OH stretch, and 3525.88 cm^{-1} assigned to the strong NH stretching of synthesized silver nanoparticles. Moreover, functional groups such as CC (alkenyl), CN (amide), *N*–H (amine) are responsible for the synthesis of nanoparticles [21]. The stabilization of developing protein-amide group encapsulation and protection against the aggregation of the CO amide band stretching [31]. Ankush et al. [6] reported similar studies, where silver nanoparticles showed functional groups such as N–H (amine), –OH (tertiary alcohol), –C–N (amine), and C–H (aromatic).

3.6.1. Scanning electron microscopy (SEM) and Energy Dispersive Spectroscopy (EDS)

The structure of the iron and silver nanoparticles was analyzed using scanning electron microscopy with EDS, as presented in Fig. 4 (a,b) and Fig. 5(a and b). The SEM results revealed cuboidal and irregular shapes for the iron nanoparticles and spherical and cuboidal shapes for the silver nanoparticles. Sirajunnisa et al. [9] reported that the shape and size of the nanoparticles depend on the nature and concentration of the used reducing agents. Furthermore, the synthesis of Fe and Ag nanoparticles using *Erodium cicutarium* plant extract revealed similar SEM images of nanoparticles with spherical morphology [12]. The energy-dispersive spectroscopy analysis of *Ricinus communis*-mediated iron and silver nanoparticles showed their elemental composition. The synthesized iron nanoparticles revealed the presence of 37% of Fe and 62% of oxygen in the sample, confirming the high purity of the iron nanoparticles. The synthesized silver nanoparticles showed that the nanoparticles held about 85% silver and 15% oxygen. Similarly, Netala et al. [32] reported that silver nanoparticles synthesized using *Flemingia wightianas* extract had a silver content of 41%.

Table 3
GC-MS analysis of methanolic extract of *Ricinus communis*.

RT	Compound	MF	Biological function
3.1494	Benzyl 2-chloroethyl sulfone	C9H11ClO2S	Odour agent
19.2396	Phosphonofluoridic acid, (1-methylethyl)-, cyclohexyl ester	C9H18FO2P	Fatty acid
23.9501	Methyl tetradecanoate	C15H30O2	Emulsifier. flavouring agent and a fragrance
25.3166	Citronellol	C10H20O	Anticonvulsant, antihyperalgesic
25.6114	4-Methoxycinnamic acid, TMS derivative	C13H18O3Si	Antoi oxidant, food addivte
26.4529	Hexadecanoic acid, methyl ester	C17H34O2	Antibacterial activity
28.5328	Methyl 12,13-octadecadienoate	C19H34O2	Fatty acid
28.5907	*N*-Hydroxy-12-azadispiro (4,1,4,2)tridec-8-ene-6,13- dione	C12H15NO3	Anti bacterialactivity
28.5981	2-Furoic acid, 4-biphenyl ester	C17H12O3	Falouring agent
28.6057	9-Octadecenoic acid, methyl ester, (E)-	C19H36O2	Anti-inflammatory, antiandrogenic, and anemiagenic, anti tumour
28.6084	Propanoicacid, 3-chloro-, 4-formylphenyl ester	C10H9ClO3	Bio oil
28.6150	1-Methyltricyclo [2.2.1.0 (2,6)]heptane	C8H12	Falouring agent
28.7391	Phytol	C20H40O	aromatic ingredient, antimicrobial, anxiolytic, metabolism-modulating, cytotoxic, antioxidant,autophagy-and apoptosis inducing, antinociceptive, anti-inflammatory,immunemodulating and neuroprotective
28.8742	Methyl stearate	C19H38O2	Emulsifier
29.3739	*p*-Cyanophenylp-(2-propoxyethoxy)benzoate	C19H19NO4	Anti microbial
29.8016	8-Methoxy-2-phenethylchromone	C18H16O3	Oil
30.3272	Arachidonoyl amide, *N*-(trifluoroacetyl)-	C22H32F3NO2	Fatty acid
30.3404	5,8,11,14-Eicosatetraenoic acid, methyl ester, (all-Z)-	C21H34O2	Anti microbial
30.4135	Santalol, cis,.alpha.-	C15H24O	Anti cancer
30.5033	Ethanol,2-(9,12-octadecadienyloxy)-, (*Z*,*Z*)-	C20H38O2	Anti microbial
30.6842	Vanadium, (.eta.7-cycloheptatrienylium)(. eta.5–2,4- cyclopentadien-1-yl)-	C12H12V	Treatment of parasitic diseases, malign tumors, bacterial and viral infections.
31.3075	9,11-Octadecadienoic acid, methyl ester, (*E*,*E*)-	C19H34O2	Fatty acid, apoptosis inducer, an antineoplastic agent, an anti-inflammatory agent, an antiatherogenic agent, a bacterial xenobiotic metabolite
31.3147	Linoleic acid ethyl ester	C20H36O2	Antileukemic, anti oxidant
32.1045	Phthalazine-1,4(2H,3H)-dione,2-(2-ethyl-6-methylphenyl)-	C17H16N2O2	Anti bacterial and anti cancer
32.6098	Pyrazol-3(2H)-one,4-(2-furfurylidenamino)-1,5-dimethyl-2-phenyl	C16H15N3O2	Anti microbial, anti cancer and anti oxidant
32.9197	Methyl 3-bromo-1-adamantaneacetate	C13H19BrO2	Aromatic compound
33.1687	Cyclotrisiloxane, hexamethyl-	C6H18O3Si3	Antioxidant and antidiabetic
33.1758	2,4(3H,8H)-Pteridinedione,6,7,8-trimethyl-	C9H10N4O2	Anti cancer
33.2920	1,3-Benzenedicarboxylicacid,5-(1,1-dimethylethyl)-	C12H14O4	*Antimicrobial and antifouling properties*
33.2972	Adamantane-1-carboxamide,N-[2-(3,4-dimethylphenoxy)ethyl]-	C21H29NO2	Chemotherapeutic agent
33.3148	3,6-Dipentyl-2,5-dimethylpyrazine	C16H28N2	Falvouring agent and anti cancer
33.3816	DL-Laudanosine	C21H27NO4	Reduce hyper tension
33.4545	Indolizine, 2-(4-methylphenyl)-	C15H13 N	Anti microbial
33.5322	Succinicacid,3-methylbut-2-yl pentafluorophenyl ester	C15H15F5O4	Food additives, detergents, cosmetics, pigments,
33.6558	3,5-Pyridinedicarboxylicacid,1,4-dihydro-4-(1-methylethyl)-, diethyl ester	C14H21NO4	Anti bacterial
33.7243	Pyrrolidine-1-carboxylicacid,2-cycloheptylaminocarbonyl-4-hydroxy-, phenyl ester	C19H26N2O4	Anti oxidant
33.7331	6,7,8-Trimethoxy-3,4-dimethyl-1-methylsulfanyl3,4-dihydroisoquinoline	C15H21NO3S	Anti inflammatory
33.8323	Terephthalicacid, butyl2-(4-nitrophenoxy)ethyl ester	C20H21NO7	Anti microbial
34.0795	Fumaric acid, di (2-fluorophenyl) ester	C16H10F2O4	Food additive
34.1270	1,2-Benzisothiazol-3-amine,TBDMS derivative	C13H20N2SSi	Anti microbial
34.3294	Papaveroline,2′-bromo-2-methyl-, tetramethyl (ester)	C21H26BrNO4	Alkaloids
34.3824	Cyclotrisiloxane, hexamethyl-	C6H18O3Si3	Antioxidant and antidiabetic activities.
34.3934	Phthalic acid,4-nitrophenyl2-propyl ester	C17H15NO6	Anti microbial, anti oxidant and anti cancer
34.5477	Quinoxaline, 2-phenyl-	C14H10N2	Antiprotozoal, antiviral, anti-inflammatory, and antibacterial and as a kinase inhibitor
34.5858	Papaveroline,2′-bromo-2-methyl-, tetramethyl (ester)	C21H26BrNO4	Analgesic,anti-inflammatory, anti-hypertensive
34.6202	L-Proline,N-(pentafluorobenzoyl)-, heptyl ester	C19H22F5NO3	Proper functioning of joints and tendons.
34.7297	Benzamidine, 4-(4-pentylphenyl)-	C18H22N2	Treat painful and inflammatory conditions of the oral cavity, such as infections and gingivitis

(*continued on next page*)

Table 3 (*continued*)

RT	Compound	MF	Biological function
34.8089	4-Quinazolinol, 2-methyl-, 3-oxide	C9H8N2O2	Anti cancer
34.9191	Thiazolidin-4-one,2-(4-methylphenylimino)-	C10H10N2OS	Antitubercular, antidiabetic, anti microbial, anti cancer
34.9364	L-Leucine, *N*-(2-chloroethoxycarbonyl)-*N*-methyl-, dodecyl ester	C22H42ClNO4	Tissue regeneration, and metabolism.
34.9900	Isophthalicacid, monoamide,N-(2-chlorophenyl)-, propyl ester	C17H16ClNO3	Fatty acid
35.0652	Cyclotrisiloxane, hexamethyl-	C6H18O3Si3	Antioxidant and antidiabetic activities.
35.3688	2,4-Dimethyl-7-chloroquinoline	C11H10ClN	Anti microbial, anti inflammatory
35.8497	Pyrrolo [1,2-a]-1,3,5-triazine-8-carbonitrile,3-ethyl1,2,3,4-tetrahydro-2,4-dioxo-7-phenyl	C15H12N4O2	Antipsychotic, β-adrenergic antagonist, anxiolytic, anticancer (leukemia, lymphoma and myelofibrosis etc.), antibacterial, antifungal, antiprotozoal, antimalarial
35.8634	Phosphineoxide, bis(pentamethylphenyl)-	C22H31OP	Anti cancer
36.1727	Pendimethalin	C13H19N3O4	Control grasses and weeds in field crops
36.1753	Scopoletin, O-acetyl-	C12H10O5	*Antihepatotoxicity, antibacterial*, antifungal
36.4809	Norreticuline, *N*-formyl-	C19H21NO5	Anticanceractivity.
36.4983	Quinoxaline, 2-phenyl-	C14H10N2	Anti microbial and anti oxidant
36.7018	3-Methylbenzothiophene	C9H8S	Anti microbial activity
36.7617	3,4-Dimethoxycinnamic acid	C11H12O4	Anti oxidant
36.8038	Carbon tetrabromide	CBr4	*Antioxidant, anti-glucosidas*
36.8591	3,6-Dinitro-1H-indole	C8H5N3O4	Anti microbial
36.9113	6-Methoxy-3-methyl-2-benzofurancarboxylic acid	C11H10O4	Anti microbial
36.9433	Methanamine,N-(1-[1,1′-biphenyl]-2-ylethylidene)-	C15H15 N	Antimicrobial activity
37.0202	1-Triethylsilyloxyheptadecane	C23H50OSi	Anti bacterial
37.2594	Egenine	C20H19NO6	*Antimicrobial and antineoplastic activities*
37.5664	Clopidol	C7H7Cl2NO	Antiplatelet agent
37.7724	Isoelemicin	C12H16O3	*Antibacterial and antioxidant activity*

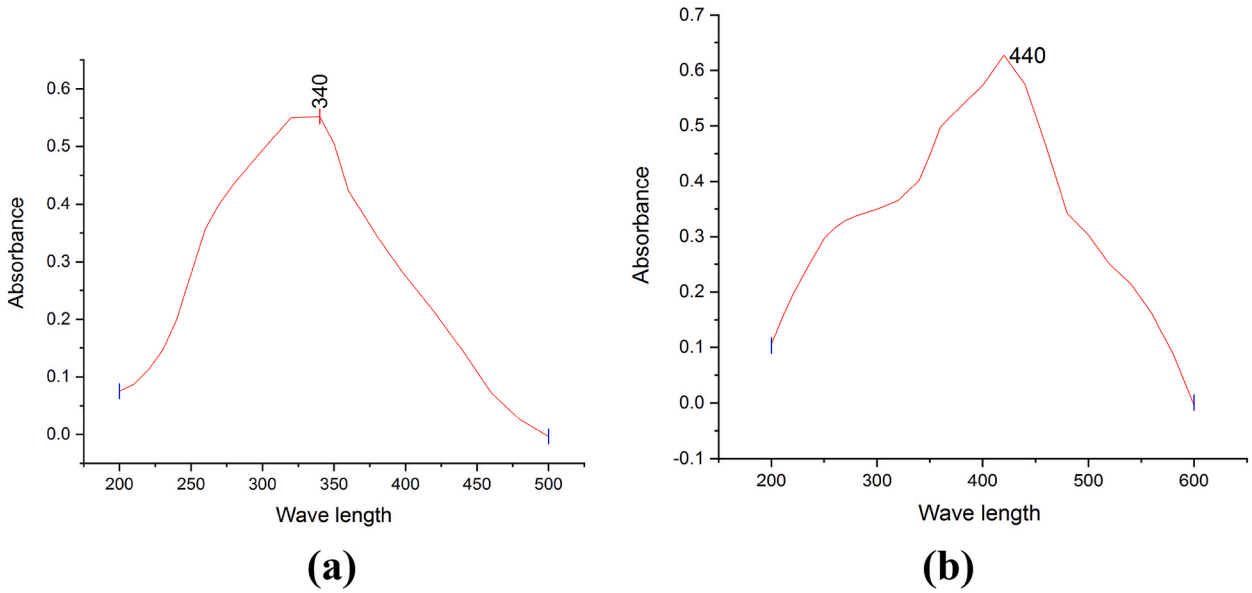

Fig. 2. UV–Vis spectral analysis of (a) FeNPs and (b) AgNPs.

3.7. X-Ray Diffraction (XRD)

The XRD analysis revealed that the synthesized iron and silver nanoparticles had intensive and strong peaks at 2θ values around 35° and 38°, as shown in Fig. 6 (a,b). Rajathirajan et al. [5] reported that the crystalline nature and composition of iron nanoparticles were evaluated using XRD diffraction with Bragg's angle ranging in the range of 20–80° at 2θ. The peaks, with their position and relative intensity, of the nanoparticles were adaptable with the crystalline nature of the silver and indicated that nanoparticles were formed to produce silver nanoparticles [33]. In similar studies, green-synthesized iron and silver nanoparticles showed diffraction peaks at 2θ values around 33° and 38°, respectively [24]. The Debye-Scherrer's equation, with Scherrer's constant 0.9, was used to estimate the average size of the crystallite, which was found to be 6.19 nm [9]. Sajedeh et al. [11] reported that the iron nanoparticles were amorphous and had broadened peaks at 20–30 °C, related to organic compounds, due to their lack of distinct diffraction peaks.

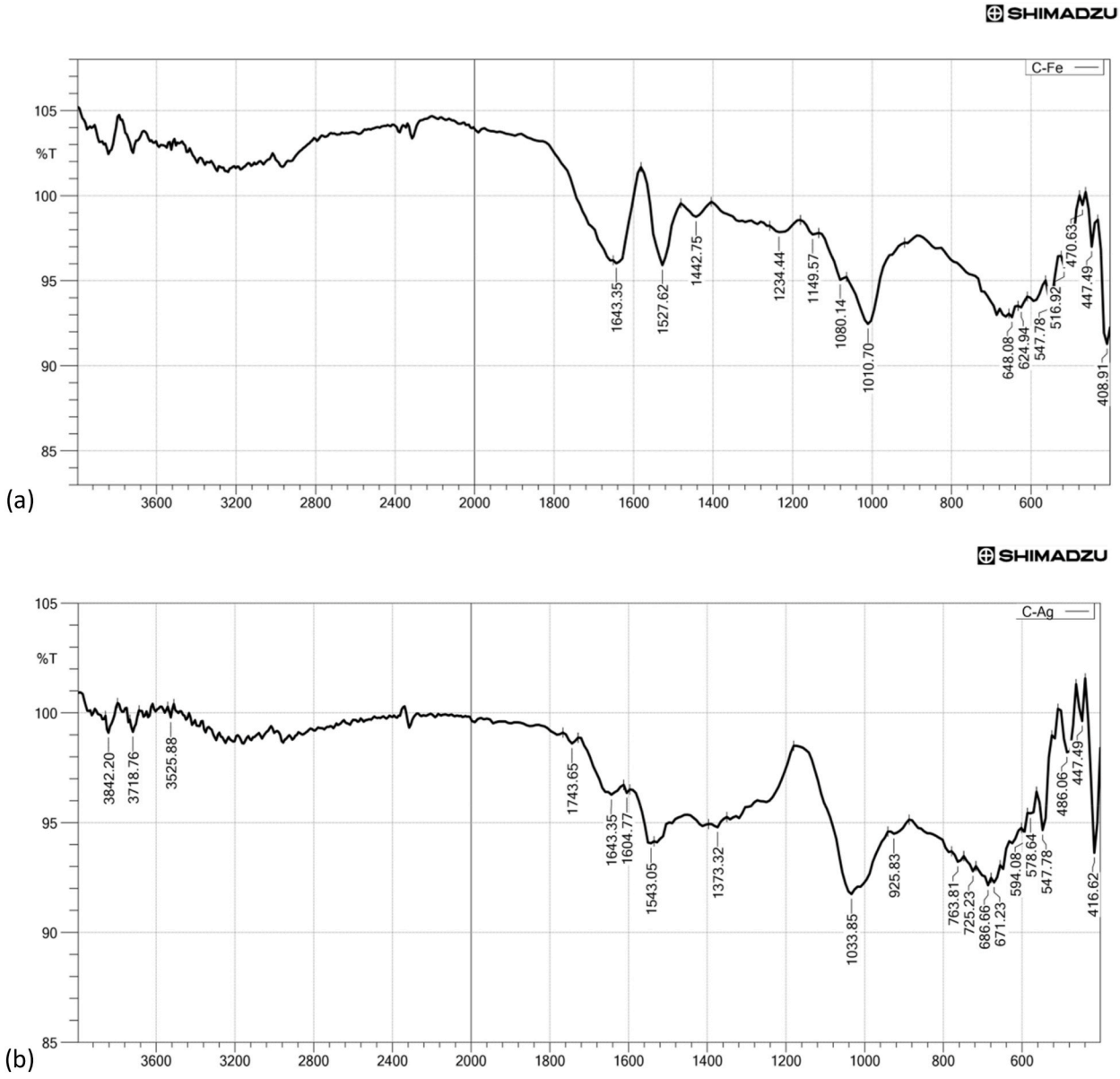

Fig. 3. FT-IR analysis of synthesized (a) FeNPs and (b) AgNPs.

3.8. Transmission electron microscopy (TEM) analysis

Transmission electron microscopy (TEM) analysis was used to investigate the morphology of the synthesized iron and silver nanoparticles, as shown in Fig. 7(a and b). The TEM micrographs showed that the green-synthesized iron nanoparticles were spherical and cuboid in shape, with a size range of 50 nm. These findings were consistent with previous studies. The TEM image of iron nanoparticles revealed that the nanoparticles were spherical in shape, with a size of ~70–100 nm [34]. Prodan et al. [35] reported similar results from TEM pictures of iron nanoparticles, showing a spherical morphology with an average size of the nanoparticles being 7 ± 0.2 nm. The TEM image of silver nanoparticles showed morphology of spherical and round shapes with an average particle size of 50 nm. The present findings are similar to those of biosynthesized silver nanoparticles, which are spherical in shape with sizes ranging between 20 and 40 nm [32]. Silver nanoparticles synthesized using extracts from three medicinal plants, *M. balbisiana*, *A. indica*, and *O. tenuiflorum*, showed that spherical shapes were predominant, with sizes up to 200 nm [36]. Moreover, the TEM micrographs of green-synthesized silver nanoparticles using medicinal plant *Lonicera japonica* leaves extract have been reported, clearly showing the original spherical morphology of AgNPs [37].

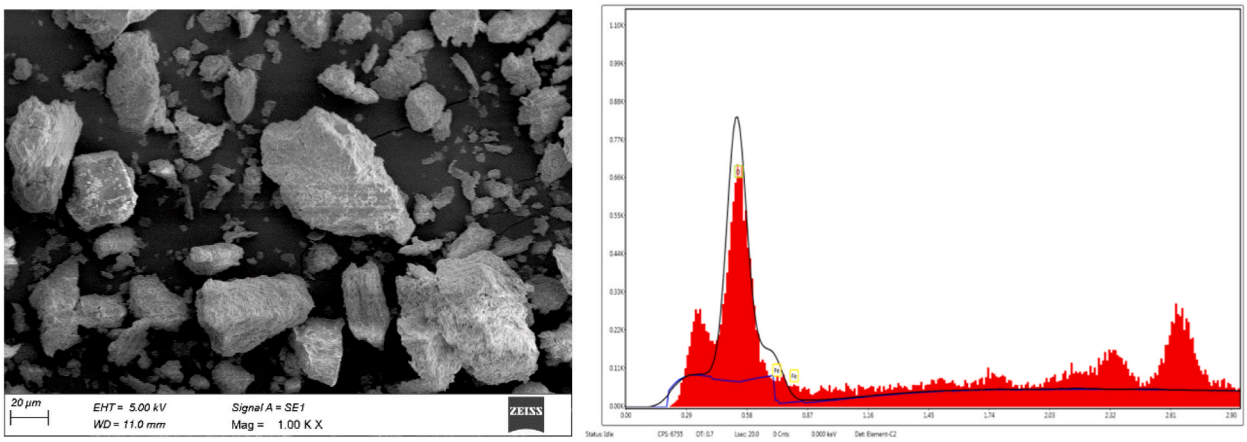

Fig. 4. SEM and EDS-FeNPs.

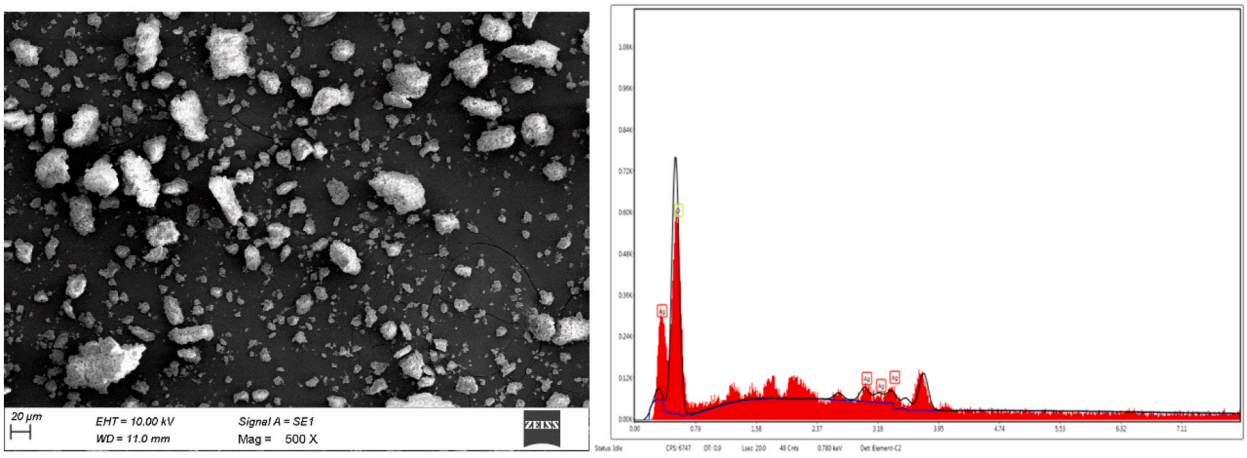

Fig. 5. SEM and EDS-AgNPs.

3.9. In vitro studies

3.9.1. Antibacterial activity of iron and silver nanoparticles

The antibacterial activity of *Ricinus communis*-mediated iron and silver nanoparticles revealed activity against human pathogenic bacteria, with a maximum inhibition zone for *Salmonella typhi* (6 ± 0.073) and (7 ± 0.040), *Staphylococcus aureus* (5 ± 0.086) and (6 ± 0.017), and *Escherichia coli* (2 ± 0.034) and (3 ± 0.052) as shown in Fig. 8 and Table 4. These inhibition zone results indicate that the iron and silver nanoparticles have strong antibacterial activity. The difference in inhibition is due to the cell wall arrangement in gram-positive and gram-negative pathogens [33]. As a result, the antibacterial activity is consistent and effective with green-synthesized iron and silver nanoparticles in different plant extracts reported in earlier studies [10,38,39]. The antibacterial potential of biogenic iron nanoparticles synthesized from spinach leaves extract against *B. subtilis* (23.56 ± 1.00) and *E. coli* (20.33 ± 0.58) were reported [40]. Silver nanoparticles showed prominent antibacterial activity, with a zone of inhibition found in the case of *E. coli* (17.00 ± 0.14 mm), *Shigella* sp. (18.00 ± 0.21 mm), *Salmonella typhi* (14.00 ± 0.13 mm), and *Listeria* sp. (13.00 ± 0.29 mm) [6]. The present study concluded that the synthesized AgNPs promised better antimicrobial activity against *Staphylococcus aureus* and *Salmonella typhi* when compared to the plant extract. The nanoparticles are characterized by a highly developed surface and small particle size, which increases their antimicrobial effect [36]. Depending on their charge and surface chemistry, nanoparticles interact with lipids, hydrophobicity, and proteins of the bacterial cell membrane [41]. Studies have confirmed the capability of silver nanoparticles biosynthesized using plant extracts of *Salvia spinosa* grown *In vitro* [42]. Faisal et al. [43] reported on the toxicity of the biosynthesized nanoparticles on human PMBCs in in vitro experiments. The absence of toxicity in nanoparticles provides more stability for subsequent pharmaceutical and other medical applications.

3.9.2. Antifungal activity of iron and silver nanoparticles

The *Ricinus communis* leaves extract-mediated iron and silver nanoparticles have significant antifungal activity against *Aspergillus*

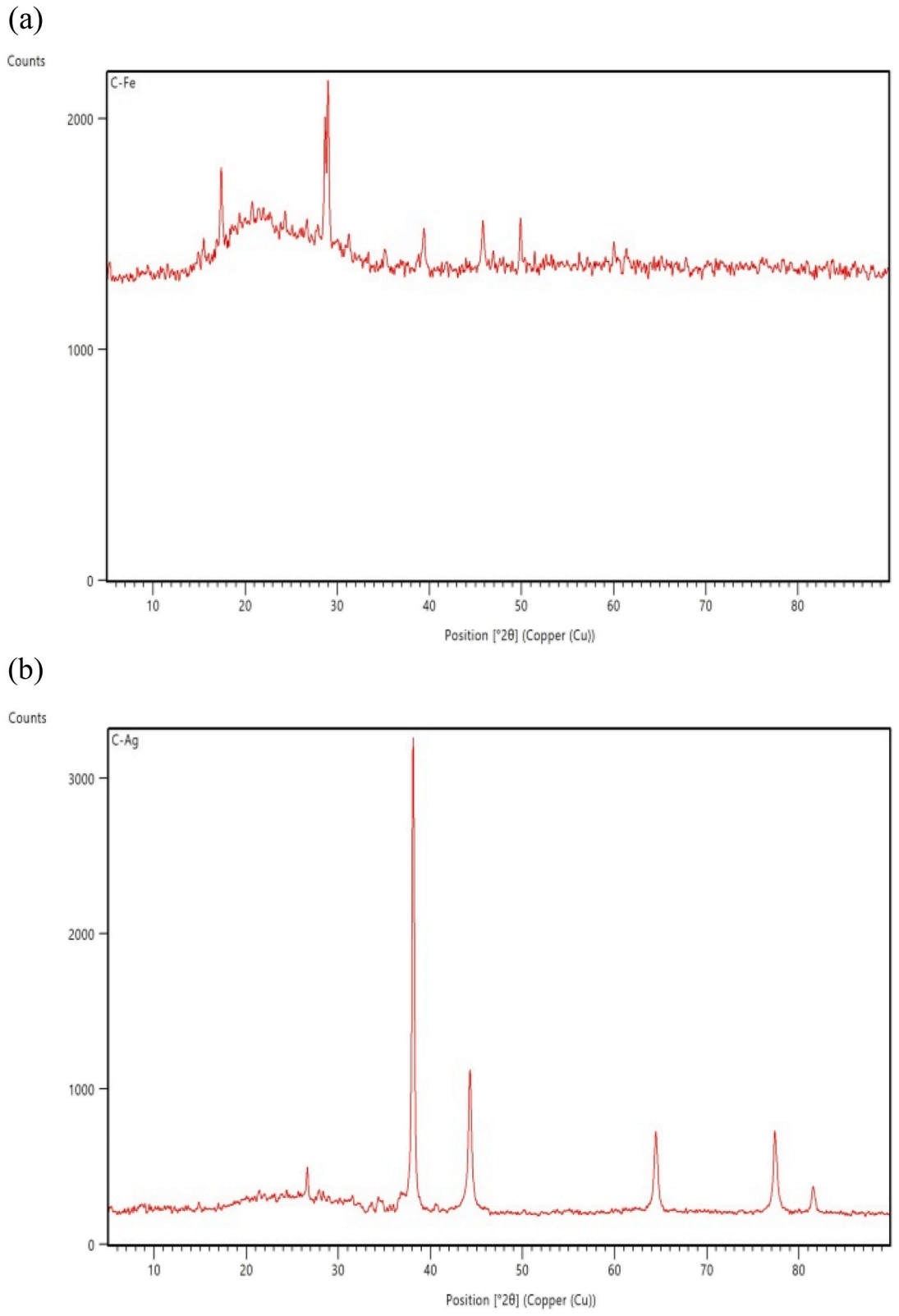

Fig. 6. XRD analysis of (a) FeNPs and (b) AgNPs.

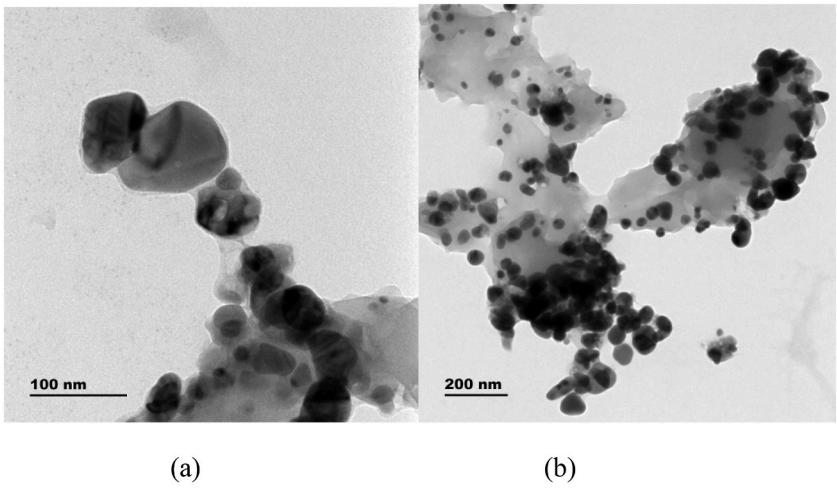

Fig. 7. TEM analysis – (a) FeNPs and (b) AgNPs.

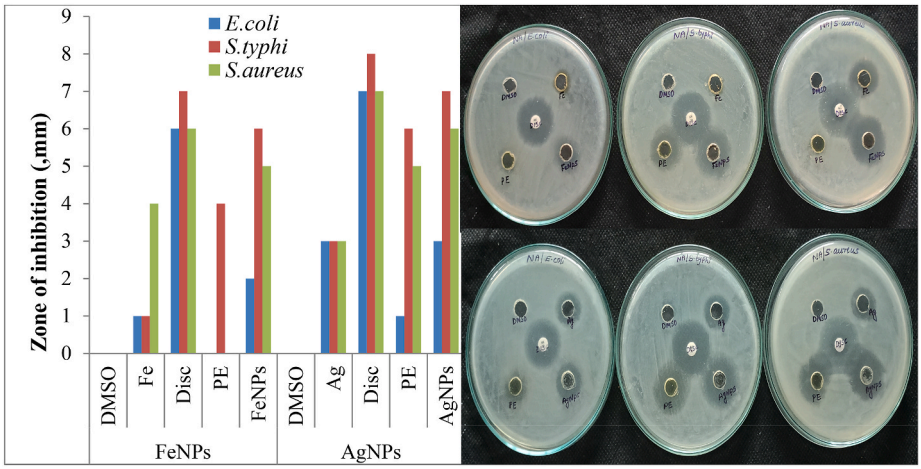

Fig. 8. Antibacterial activity of iron and silver nanoparticles against *Escherichia coli*, *Salomonella typhi* and *Staphylococcus aureus*.

Table 4
Antimicrobial efficiency of FeNPs and AgNPs.

Bacteria and Fungus	Zone of inhibition (mm)	
	FeNPs	AgNPs
E.coli	2 ± 0.034	3 ± 0.052
S.typhi	6 ± 0.073	7 ± 0.040
S.aureus	5 ± 0.086	6 ± 0.017
A.flavus	3 ± 0.042	1 ± 0.017
A.niger	1 ± 0.019	0 ± 0.019

flavus and *Aspergillus niger*, as depicted in Fig. 9 and Table 4. The synthesized iron and silver nanoparticles showed activity against *Aspergillus flavus* (3 ± 0.042) and (1 ± 0.017) and *Aspergillus niger* (1 ± 0.019) and (0 ± 0.01), respectively. However, fungi have a strong cell wall that prevents growth and being killed [33]. Rajathirajan et al. [5] reported that the antifungal activity of iron nanoparticles clearly indicated the maximum inhibition zone, which depended on the concentration of iron nanoparticles and the corresponding spore concentration of the fungi. Similarly, the green synthesis of silver nanoparticles by *Allium fistulosum*, *Tabernaemontana divaricata*, and *Basella alba* leaf extract for antifungal activity exhibited a maximum inhibition zone [44].

3.9.3. MIC (minimum inhibitory concentration)

The antibacterial activity of the synthesized iron and silver nanoparticles of *Ricinus communis* was evaluated against *Staphylococcus*

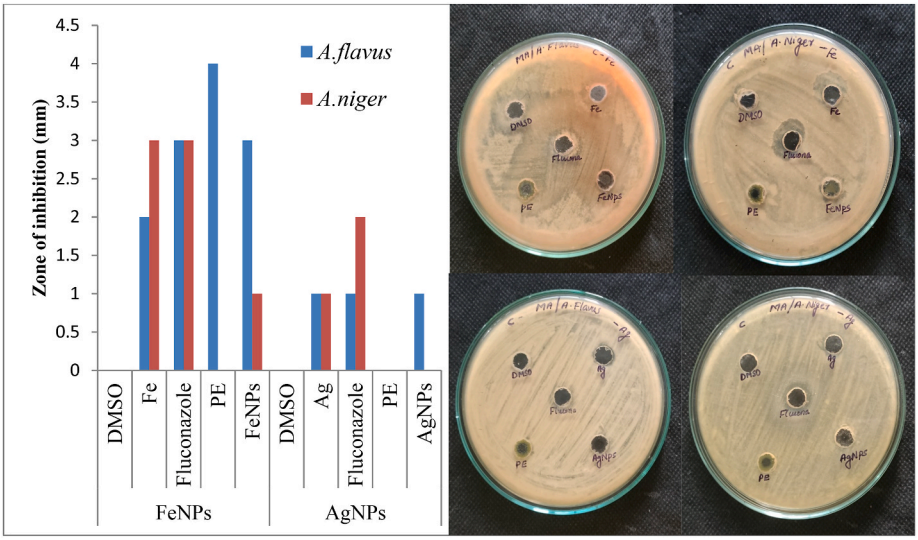

Fig. 9. Antifungal activity of iron and silver nanoparticles against *Aspergillus niger* and *Aspergillus flavus*.

aureus by determining the minimum inhibitory concentration (MIC) and cell death percentage (Fig. 10). The results showed that the iron nanoparticles exhibited the lowest and highest MIC values of 63.09% and 26.67%, respectively. The MIC values for silver nanoparticles were found to be 74.18% and 89.27%, respectively. These results indicate that the lowest concentration of iron nanoparticles dramatically inhibited bacterial growth, and this effect was more pronounced on *Staphylococcus aureus* [45]. Previous studies have reported MIC values of 10.67 ± 0.94 and 17.33 ± 1.89 μg/mL for silver nanoparticles against *Staphylococcus aureus* [46].

4. Conclusion

In this study, iron and silver nanoparticles were successfully synthesized using *Ricinus communis* leaves extract. The characterization of the synthesized nanoparticles by UV–Visible Spectroscopy, FT-IR, SEM with EDS, XRD and TEM analysis revealed strong absorbance peaks at 340 nm and 440 nm, a crystalline nature, and a well-dispersed, well-defined shape. A novel study of GC-MS analysis clearly demonstrated the phytoconstituents of *Ricinus communis* that mediated the formation of iron and silver nanoparticles, which are important for biomedical applications. From these studies, it was found that the biosynthesized nanoparticles have a broad spectrum of potential antimicrobial activity and their minimum inhibitory concentration (MIC) was assessed. *Ricinus communis* leaf extract was found to be suitable for silver nanoparticles synthesis, which is a rare occurrence. In summary, the studies demonstrated that silver nanoparticles synthesized using *Ricinus communis* leaves extract exhibited strong antimicrobial potential when compared to the plant extract and iron nanoparticles. Based on these results, it can be concluded that these nanoparticles hold great promise as a therapeutic agent for a range of biomedical applications, particularly in the field of antimicrobial treatments.

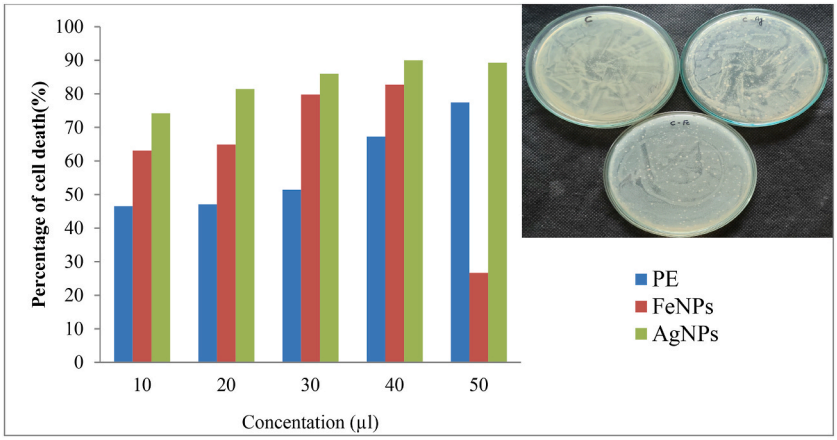

Fig. 10. Graphical representation of MIC (Values are mean at three replicates).

Author contribution statement

Linima V K: Conceived and designed the experiments; Performed the experiments; Analyzed and interpreted the data; Contributed reagents, materials, analysis tools or data; Wrote the paper. R. Ragunathan: Conceived and designed the experiments; Analyzed and interpreted the data; Contributed reagents, materials, analysis tools or data; Wrote the paper. Jesteena Johney: Conceived and designed the experiments; Analyzed and interpreted the data; Contributed reagents, materials, analysis tools or data.

Data availability statement

The authors do not have permission to share data.

Declaration of interest's statement

The authors declare no conflict of interest.

Funding statement

This research received no external funding.

Acknowledgments

This research work was supported by Centre for Bioscience and Nanoscience Research, Botanical Survey of India (Agricultural university, Tamilnadu), Vellore Institute of Technology, and PSG college of technology.

References

[1] J. Sapana, A. Rizwan, K.J. Nirmala, K.M. Rajesh, Green synthesis of nanoparticles using plant extracts, Environ. Chem. Lett. 19 (2020) 355–374.
[2] H. Imtiyaz, N.B. Singh, S. Ajey, S. Himani, S.C. Singh, Green synthesis of nanoparticles and its potential application, Biotechnol. Lett. 38 (2016) 545–560.
[3] P.B. Oladotun, B.W. Akan, U.B. Nsikak, Green synthesis of iron-based nanomaterials for environmental remediation, 1532, Environ. Nanotechnol. Monit. Manag. 13 (2020) 2215.
[4] S.K. Monika, Ponlakshmi, S.H.H. Ponlakshmi, S. Krishnan, K. Selvaraj, B. Vanavil, Fabrication of anti-bacterial cotton bandage using biologically synthesized nanoparticles for medical applications, Prog. Biomater. 11 (2022) 229–241.
[5] S.D. Rajathirajan, P. Mani, S. Palanisamy, M. Raja, S. Asad, M.E. Abdallah, S. Thangasamy, K. Woong, Nano-decolorization of methylene blue by *Phyllanthusreticulatusiron* nanoparticles: an eco-friendly synthesis and its antimicrobial, phytotoxicity study, Appl. Nanosci. 13 (3) (2021) 2527–2537.
[6] S. Ankush, S. Anand, R. Jagriti, R. Reena, Green synthesis of silver nanoparticles and its antibacterial activity using fungus *Talaromycespurpureogenus* isolated from Taxusbaccata Linn, Micro Nano Syst. Lett. 10 (2) (2022).
[7] H. Habeeb, E.T. John, Medicinal herbs as a panacea for biogenic silver nanoparticles, Bull. Natl. Res. Cent. 46 (9) (2022).
[8] D.B. Hayelom, A.W. Adhena, K.B. Hailemariam, G.A. Tekilt, Synthesis paradigm and applications of silver nanoparticles (AgNPs), Sustainable Mater. Technol. 13 (2017) 18–23.
[9] A.R. Sirajunnisa, S. Abishek, S. Sanjay, R. Geethalakshmi, S. Shanmugavel, V. Manivasagan, B.N. Ramesh, Green synthesis of iron oxide nanoparticles using *Hibiscus rosa-sinensis*for fortifying wheat biscuits, SN Appl. Sci. 2 (2020) 898.
[10] P. Rohini, H.N. Shivraj, M. Nilesh, S. Ragini, P.S. Rana, S.K. Arun, Green synthesis of silver nanoparticles using the *Tridaxprocumbensplant* extract and screening of its antimicrobial and anticancer activities, Oxid. Med. Cell. Longev. 1 (2022) 14.
[11] L. Sajedeh, A.J.K. Mohammad, B. Nasrin, G. Younes, M.A. Ali, T. Saeed, Green synthesis of iron nanoparticles using *Plantagomajor* leaf extract and their application as a catalyst for the decolorization of azo dye, BioNanoScience 9 (2019) 317–322.
[12] M. Nahid, A.A. Parviz, S.T. Mohammad, W.H. Syed, L. Kambiz, Biosynthesis of Ag and Fe nanoparticles using *Erodiumcicutarium*; study, optimization, and modeling of the antibacterial properties using response surface methodology, J. Nanostruct. Chem. 9 (2019) 203–216.
[13] S. Shalima, B. Chasan, B. Ahmet, A.K. Ishak, N.K. Isik, A. Zerrin, O.O. Mustafa, E.K. Serap, Green synthesis and characterization of silver and iron nanoparticles using *Neriumoleander*extracts and their antibacterial and anticancer activities, Plant Introd. (2021) 36–49.
[14] W. Muhammad, N. Shabab, A. Sadia, A. Muhammad, A. Bilal, A.K. Naveed, H. Bilal, K.A. Al-Ghanim, F. Al-Misned, N. Mulahim, M. Shahid, Evaluation of larvicidal efficacy of *Ricinus communis* (Castor) and synthesized green silver nanoparticles against *AedesaegyptiL*, Saudi J. Biol. Sci. 27 (2020) 2403–2409.
[15] B. Debadin, C. Someswar, Biogenic synthesis of silver nanoparticles using guava (*Psidiumguajava*) leaf extract and its antibacterial activity against *Pseudomonas aeruginosa*, Appl. Nanosci. 6 (2016) 895–901.
[16] S. Sreelakshmy, S. Thangapandiyan, *In vitro* antibacterial efficacy of *Plectranthusamboinicus* mediated silver nanoparticles against urinary tract pathogens, Asian J. Pharmaceut. Clin. Res. 12 (2) (2019) 153–159.
[17] K.P. Anjali, B.M. Sangeetha, R. Ragunathan, G. Devi, S. Dutta, Seaweed mediated fabrication of zinc oxide nanoparticles and their antibacterial, antifungal and anticancer applications, ChemistrySelect 6 (4) (2021) 647–656.
[18] S.M. Edwin, G.K. Patrick, G.M. Ernest, O.N. Augustine, I.W. Sammy, O.N. Jared, Biosynthesis of iron nanoparticles using *Ageratum conyzoides* extracts, their antimicrobial and photocatalytic activity, SN Appl. Sci. 1 (2019) 500.
[19] R.N. Vasudeva, S.K. Venkata, N. Venkateswarlu, B. Pushpalatha, B.G. Sukhendu, T. Vijaya, First report of biomimetic synthesis of silver nanoparticles using aqueous callus extract of *Centellaasiatica*and their antimicrobial activity, Appl. Nanosci. 5 (2015) 801–807, https://doi.org/10.1007/s13204-014-0374-6.
[20] F. Somayeh, J. Mina, Y. Mohammad, Biologically synthesized silver nanoparticles by aqueous extract of *Saturejaintermedia* C.A. Mey and the evaluation of total phenolic and flavonoid contents and antioxidant activity, J Nanostruct Chem 6 (2016) 357–364, https://doi.org/10.1007/s40097-016-0207-0.
[21] A.M. Awwad, N.M. Salem, A.O. Abdeen, Green synthesis of silver nanoparticles using carob leaf extract and its anti-bacterial activity, Int. J. Ind. Chem. 4 (2013) 1–6.
[22] J. Jesteena, S.S. Radhai, R. Ragunathan, Extraction of chitin and chitosan from wild type *Pleurotus*Spp and its potential application innovative approach, J. Pure Appl. Microbiol. 12 (3) (2018) 1631–1640.
[23] I. Wiegand, K. Hilpert, R.E.W. Hancock, Agar and broth dilution methods to determine the minimal inhibitory concentration (MIC) of antimicrobial substances, Nat. Protoc. 3 (2) (2008) 163–175.
[24] P.S. Kiran, S.R. Dheeraj, D.B. Somnath, A.B. Mangesh, H.W. Ganesh, R.J. Namdeo, Green synthesis of silver and iron nanoparticles of isolated proanthocyanidin: its characterization, antioxidant, antimicrobial, and cytotoxic activities against COLO320DM and HT29, J. Genet. Eng. Biotechnol. 18 (43) (2020).

[25] H.L. Ayomide, A.D. Oyinade, D.T. Augustine, Green synthesis and characterization of silver nanoparticles using *Morinda lucida* leaf extract and evaluation of its antioxidant and antimicrobial activity, Chem. Pap. 76 (2022) 7313–7325.
[26] M.B. Ulewicz, M. Wesolowski, Total phenolic contents and antioxidant potential of herbs used for medical and culinary purposes, Plant Foods Hum Nutr 74 (1) (2019) 61–67.
[27] A. Tanvir, S.K.M. Rahman, M.S. Abdullah, Thin layer chromatographic profiling and phytochemical screening of six medicinal plants in Bangladesh, Int. J. Biosci. 11 (1) (2017) 2222–5234.
[28] K.K. Lakshmi, D. Akalanka, K. Satyavathi, P. Bhojaraju, GC-MS analysis of bio-active compounds in methanolic extract of *Lactucaruncinata* DC, Pharmacogn. Res. 6 (1) (2013).
[29] V. Vorobyova, G. Vasyliev, M. Skiba, Eco-friendly "green" synthesis of silver nanoparticles with the black currant pomace extract and its antibacterial, electrochemical, and antioxidant activity, Appl. Nanosci. 10 (12) (2020) 4523–4534.
[30] K. Sravanthi, D. Ayodhya, S. Yadgiri, Green synthesis, characterization of biomaterial-supported zero-valent iron nanoparticles for contaminated water treatment, J. Anal. Sci. Technol. 9 (3) (2018).
[31] K. Mujahid, W. Pundlik, S. Navinchandra, Synthesis of Zno nanoparticles using peels of passiflorafoetida and study of its activity as an efficient catalytic for the degradation of hazardous organic dye, SN Appl. Sci. 3 (2021) 528.
[32] V.R. Netala, M.S. Bethu, S. Sana, P. Duggina, K.V. Subbaiah, V. Tartte, Eco-friendly synthesis of silver nanoparticles using leaf extract of *Flemingiawightiana*: spectral characterization, antioxidant and anticancer activity studies, SN Appl. Sci. 2 (2020) 884.
[33] S. Rajeshkumar, *Citrus Lemon* juice mediated preparation of AgNPs/Chitoson based bionanocomposites and its antimicrobial and antioxidant activity, J. Nanomater. (2021) 1–10.
[34] A. Abdulaziz, S.A. Mohammed, M. Ayesha, M.A. Kalam, A. Abdullah, A. Raisuddin, K. Mohsin, M.A. Khalid, S. Rabbani, Iron oxide nanoparticles: preparation, characterization, and assessment of antimicrobial and anticancer activity, Adsorpt. Sci. Technol. (2022) 1–9.
[35] A.M. Prodan, S.L. Iconaru, C.M. Chifiriuc, B. Coralia, C.S. Ciobanu, M. Mikael, S. Stanislas, P. Daniela, Magnetic properties and biological activity evaluation of iron oxide nanoparticles, J. Nanomater. 1 (2013) 7.
[36] K. Anna, S. Mateusz, K. Eva, R. Jacek, L. Anna, G.B. Ploskonska, Similarities and differences between silver ions and silver in nanoforms as antibacterial agents, Int. J. Mol. Sci. 19 (2) (2018) 444.
[37] G.N. Rajivgandhi, C. Gnanasekaran, R. Govindan, M. Natesan, R. Ragunathan, M.Z. Siddiqi, N.S. Alharbi, J.M. Khaled, L. Wen-Jun, Synthesis of silver nanoparticles (Ag NPs) using phytochemical rich medicinal plant *Lonicera japonica* for improve the cytotoxicity effect in cancer cells, J. King Saud Univ. Sci. 34 (2022).
[38] V. Yosmery, F. Maice, C. Maria, C. Carlos, Synthesis of iron nanoparticles from aqueous extract of *Eucalyptus robusta*Sm and evaluation of antioxidant and antimicrobial activity, Mater. Sci. Energy Technol. 3 (2020) 97–103.
[39] S.H. Bhuiyan Md, Y.M. Muhammed, C.P. Shujit, D.A. Tutun, S. Otun, M. Rahman Md, J.I. Sharif Md, H. Ommay, Ashaduzzaman Md, Green synthesis of iron oxide nanoparticle using *Carica papaya* leaf extract:application for photocatalytic degradation of remazol yellow RR dye and antibacterial activity, Heliyon 6 (2020) EO4603.
[40] P.K. Tyagi, G. Smridhi, T. Shruti, K. Manoj, R. Pandiselvam, S.D. Dastan, S. Javad, G. Deepak, A. Arvind, Green synthesis of iron nanoparticles from spinach leaf and banana peel aqueous extracts and evaluation of antibacterial potential, J. Nanomater. (2021) 1–11.
[41] D.P. Linklater, V.A. Baulin, X.L. Guevel, J. Fleury, E. Hanssen, T.H.P. Nguyen, S. Juodkazis, G. Bryant, R.J. Crawford, P. Stoodley, Antibacterial action of nanoparticles by lethal stretching of bacterial cell membranes, Adv. Mater. 32 (52) (2020).
[42] P. Saba, G. Maryam, B. Saeid, Green synthesis of silver nanoparticles using the plant extract of *Salvia spinosa* grown in vitro and their antibacterial activity assessment, J. Nanostruct. Chem. 9 (2019) 1–9.
[43] N. Faisal, F. Fozia, A. Madeeha, A. Ijaz, A. Shakeel, U. Riaz, M.H. Almutairi, A. Lotfi, M.M. Abdel-Daim, Characterization, antiplasmoidal and cytotoxic activities of green synthesized iron oxide nanoparticles using *Nephrolepis exaltata* aqueous extract, Molecules 27 (2022) 4931.
[44] S. Vinodhini, B.S.M. Vithiya, T.A.A. Prasad, Green synthesis of silver nanoparticles by employing the *Allium fistulosum*, *Tabernaemontana* divaricate and *Basella alba* leaf extracts for antimicrobial applications, J. King Saud Univ. 34 (2022).
[45] S.A. Leili, A. Vahid, A.M. Tamaddon, A.M. Amani, T. Saeed, Green synthesis of iron-based nanoparticles using *Chlorophytumcomosum* leaf extract: methyl orange dye degradation and antimicrobial properties, Heliyon 7 (2021).
[46] M.A. Ansari, M.A. Alzohairy, One-pot facile green synthesis of silver nanoparticles using seed extract of *Phonixdactylifera* and their bactericidal potential against MRSA, Evid. base Compl. Alternative Med. (2018) 1–9.